Distribution Agreement

In presenting this thesis as a partial fulfillment of the requirements for a degree from Emory University, I hereby grant to Emory University and its agents the non-exclusive license to archive, make accessible, and display my thesis in whole or in part in all forms of media, now or hereafter known, including display on the world wide web. I understand that I may select some access restrictions as part of the online submission of this thesis. I retain all ownership rights to the copyright of the thesis. I also retain the right to use in future works (such as articles or books) all or part of this thesis.

Signature:

Abhinav Kumar Sharma 04/16/2014

Ultrasensitive detection of glioblastoma brain tumor cells using 5-ALA and SpectroPen for fluorescence-guided resection

By

Abhinav K. Sharma

Dr. Shuming Nie

Advisor

Neuroscience and Behavioral Biology Program

Dr. Shuming Nie

Advisor

Dr. Leah Roesch

Committee Member

Dr. George Wilmot

Committee Member

Dr. Fahim Atif

Committee Member

Dr. Brad Kairdolf

Non-Voting Committee Member

2014

Ultrasensitive detection of glioblastoma brain tumor cells using 5-ALA and SpectroPen for fluorescence-guided resection

By

Abhinav K. Sharma

Dr. Shuming Nie

Advisor

An abstract of

A thesis submitted to the Faculty of Emory College of Arts and Sciences

Of Emory University in partial fulfillment

Of the requirements of the degree of

Bachelor of Sciences with Honors

Neuroscience and Behavioral Biology Program

2014

Abstract

By Abhinav K. Sharma

SpectroPen is a handheld spectrometer that can be used intraoperatively to help surgeons detect glioblastoma tumor cells, therefore maximizing tumor cell resection by helping surgeons delineate diffuse and undefined tumor margins that are characteristic of glioblastoma. The use of a metabolic contrast agent, 5-aminolevulinic acid (5-ALA), is also tested as a means by which the SpectroPen can selectively detect fluorescence in cancer cells through the tumor cell-specific accumulation of protoporphyrin-IX (Pp-IX), a fluorescent metabolite of the 5-ALA prodrug. Here, we show that SpectroPen is capable of detecting fluorescence emission from Pp-IX *in vitro* with U87 EGFRvIII glioblastoma cells lines as well as from Pp-IX in tumor cells within xenograft mice models that have had U87 EGFRvIII tumor cell implantation in their brains. Additionally, the device has shown much greater sensitivity to fluorescence emission from tumor cells than the more conventional surgical fluorescent microscope, as seen by SpectroPen's detection threshold of 2,500 U87 EGFRvIII cells. My project demonstrates the efficacy of 5-ALA as a contrast agent in staining studies using U87 EGFRvIII tumor cells and normal cell lines, astrocytes and NIH/3T3, via tests for selective uptake and fluorescence in the U87 EGFRvIII cells. The results obtained from these studies are currently being translated to the clinic, where we are collaborating with Dr. Costas Hadjipanayis of Emory University Hospital Midtown. Currently, 5-ALA is not approved by the FDA in the United States and thus Dr. Hadjipanayis is currently performing Phase II clinical trials with the drug.

Ultrasensitive detection of glioblastoma brain tumor cells using 5-ALA and SpectroPen for fluorescence-guided resection

By

Abhinav K. Sharma

Dr. Shuming Nie

Advisor

A thesis submitted to the Faculty of Emory College of Arts and Sciences

Of Emory University in partial fulfillment

Of the requirements of the degree of

Bachelor of Sciences with Honors

Neuroscience and Behavioral Biology Program

2014

Acknowledgements

First and foremost, I would like to dedicate this thesis to my dear Guru, Jagadguru Kripaluji Maharaj, without whom I would not be in the position that I am today. I am eternally grateful for the grace He has bestowed upon me. Through tough times and long nights, I know that I have had Lord Krishna watching over me and guiding me every step of the way, and this thesis is but a small, yet significant, part of the journey. I would like to thank my parents for their endless support and for all of their sacrifices. Mom, Dad, thank you from the bottom of my heart for doing whatever it took to make sure I received the best education possible. Everything I have done, I have done to make you proud. Additionally, I am incredibly grateful to Dr. Shuming Nie and Dr. Brad Kairdolf for their mentorship and their support over the past few years. Dr. Nie, I am forever appreciative of the opportunity you gave me, as a freshman back in 2011, to work in your lab. You have been very supportive and have always volunteered to help out in any way you could. Brad, where do I begin? Without your help, I most definitely would not be the young scientist I am today, with a job at the NIH lined up and with plans to remain in the field post-graduation. You truly have inspired me to continue doing research; from helping me make my first poster presentation to editing my oral presentations and honors thesis, you have been an immense help in my scientific career thus far. Lastly, I would like to send a massive shout-out to family members, friends, professors, and mentors (including my thesis committee members) who have been there for me, and who have supported me throughout my time at Emory and even before my arrival at college. I could not have made it to this point without your words of encouragement.

TABLE OF CONTENTS

LIST OF FIGURES

LIST OF TABLES

INTRODUCTION

Malignant gliomas are the most common and deadly brain tumors (Van Meir et al., 2010). The current standard of care involves the orally-administered drug temozolomide along with radiotherapy and surgical debulking (Stupp et al., 2005). For highly aggressive cancers such as glioblastoma, it is of prime importance to eradicate as many tumor cells as possible: tumor recurrence corresponds closely to cancer cells left in the body (Lacroix et al., 2001). Intraoperative delineation of tumor boundaries and peripheral cells from normal cells and tissue using conventional technology is a challenging task for surgeons, as is identifying cancerous nodules and lymph nodes (Vahrmeijer et al., 2013). Fluorescent contrast agents, however, allow for intraoperative visualization of cancerous tissue, thereby allowing for quick and accurate detection of tumorous tissue (Vahrmeijer et al., 2013).

This project involves testing a device called SpectroPen (Figure 1), which is a handheld spectrometer that can be used during surgical intervention for fluorescence-guided resection of malignant gliomas (Mohs et al., 2010). In comparison with conventional fluorescence surgical microscopes used in the operating room, the system has a number of key design advantages (short working distance, algorithm-assisted spectral curve fitting) that result in greater, more sensitive visualization of glioblastoma cell fluorescence. Moreover, this project examines the efficacy of using a metabolic contrast agent for fluorescence-guided surgery (FGS) as opposed to more traditional dyes used for glioblastoma resection, such as indocyanine green (Hansen et al., 1993) (Figure 20) and fluorescein (Shinoda et al., 2003) (Figure 21).

Figure 1. Handheld Spectrometer, SpectroPen. Handheld spectrometer allows for greater mobility and proximity to tissue (Mohs et al., 2010).

5-aminolevulinic acid (5-ALA) (Figure 4) is hypothesized to be a more optimal contrast agent for FGS than indocyanine green (ICG) or fluorescein due to the fact that it is not fluorescent. Rather, it is the endogenously formed protoporphyrin-IX (Pp-IX) (Figure 5), a metabolite of 5-ALA, that is fluorescent and selectively accumulates, in photosensitizing concentrations, in tumor cells (Kennedy et al., 1990). The non-fluorescent precursor, 5-ALA, is transported into cells, of which many types appear to have distinct uptake systems (Rodriguez et al., 2006). 5-ALA is small enough to diffuse from the blood to the brain (Ennis et al., 2003), and permeate the blood-brain barrier (Jouyban et al., 2012) where it is intracellularly metabolized to Pp-IX (Duffner et al., 2005). Moreover, transportation of 5-ALA from blood to choroid plexus relies upon the PEPT2 carrier and an organic transporter (Novotny et al., 2000).

The endogenous protoporphyrin-IX is excited by violet light (~400 nm) and subsequently emits red fluorescence with characteristic peaks at 635 nm and 704 nm (Stummer et al., 1998). This emission is detected by SpectroPen, which graphs the

characteristic peaks on a monitor, allowing the surgeon to detect and confirm the precise boundaries of the tumor mass (a peak in the 630 nm range of the spectrum would indicate the presence of a tumor cell that accumulates protoporphyrin-IX). Thus, protoporphyrin-IX fluorescence is used as an intraoperative indicator of the location of tumor cells and the tumor's poorly-defined margins.

In contrast to ICG, fluorescein and other contrast agents that are passively tumor-localizing, the use of 5-ALA relies upon the selective accumulation of the fluorescent Pp-IX metabolite in cancerous cells and the conversion of Pp-IX to non-fluorescent heme in normal tissue. Significant accumulation of Pp-IX should not occur in normal cells upon administration of 5-ALA due to their ability to metabolize Pp-IX to heme (Figure 3); thus, normal cells should not fluoresce. Conversely, in tumor cells, there are errors in the heme biosynthesis pathway that result in the accumulation of the fluorescent, Pp-IX molecule (Figure 3). As a result of this preferential accumulation, Pp-IX can be excited by 405 nm light, resulting in selective fluorescence emanating from tumorous tissue. Therefore, the mechanism through which 5-ALA works as a contrast agent results in its improved signal-to-noise for tumor cell detection, relative to other, more traditional dyes.

Absorption of visible light in tissue occurs readily in large part due to melanin, hemoglobin, oxyhemoglobin, and water (Tuchin, 2000); thus light at the appropriate wavelength is very capable of exciting photosensitizers such as Pp-IX, ICG, or fluorescein. In tissue, the penetration depth of light is typically 10-20 mm (Smith et al., 2009) but varies within this range depending on the irradiating light's wavelength (Richards-Kortum & Sevick Muraca, 1996). There is an optical window of light wavelengths ("First Window," Figure 2) in live biological tissue, between 650-950 nm, at

which light propagation is relatively less attenuated by absorption and scattering in tissue (Smith et al., 2009). The most optimal window of light wavelengths, however, is in the near-infrared ("Second Window," Figure 2), at 1,000-2,500 nm (Smith et al., 2009). Near-infrared light has even greater penetration of tissue than visible light due to its longer wavelength, which results in decreased absorption and scattering within the tissue (Smith et al., 2009). Thus, for FGS it is crucial to use a contrast agent that emits fluorescence within this range of wavelengths, in order to prevent attenuation of fluorescence emission intensity from tumor cells and a subsequent decrease in detection sensitivity of tumor cells.

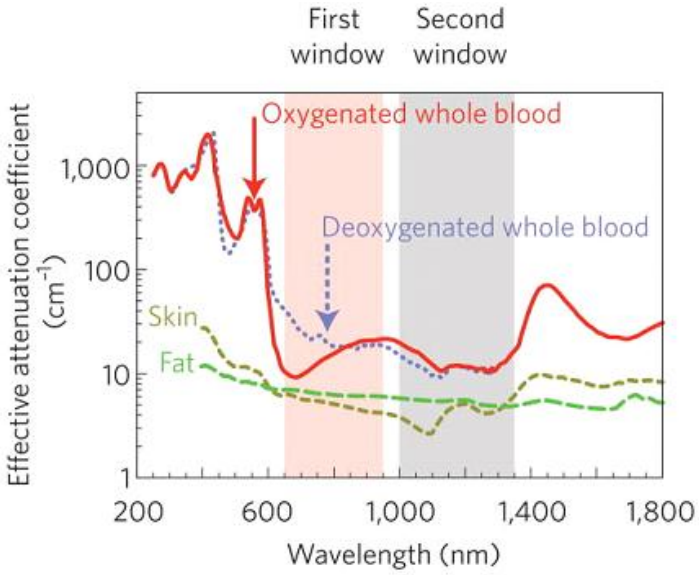

Figure 2. Attenuation of Light Intensity in Biological Tissue for 200-1,800 nm Wavelengths of Light. Longer wavelengths result in less scattering and absorption of light in biological tissues, to a certain extent. There are two optical windows of light wavelengths for imaging tissue, due to decreased attenuation of light intensity. The "Second window" corresponds to near-infrared wavelengths, which have greater light transmission than the "First window," within which light is transmitted very effectively as well. Beyond the "Second window," there is increased absorption by water and lipids and thus increased attenuation of light intensity (Smith et al., 2009).

Different contrast agents, with their respective excitation and emission wavelength properties, thus have distinct tissue penetration depth profiles. 5-ALA is more favorable than fluorescein for FGS because Pp-IX is capable of greater tissue penetration depth due to the fact that the emission wavelength of Pp-IX is longer, 630-700 nm (red fluorescence); it has increased penetration depth relative to dyes which emit at lower wavelengths (blue/green fluorescence). Emission at shorter wavelengths results in increased light absorption in tissue and light wave scattering, thus reducing detectable fluorescence intensity (Acerbi et al., 2013). Relative to ICG, however, Pp-IX fluorescence emission has less tissue penetration due to its shorter wavelength. The longer, near-infrared wavelength range of ICG's fluorescence emission cannot be detected by the eye, and can only be visualized with camera systems.

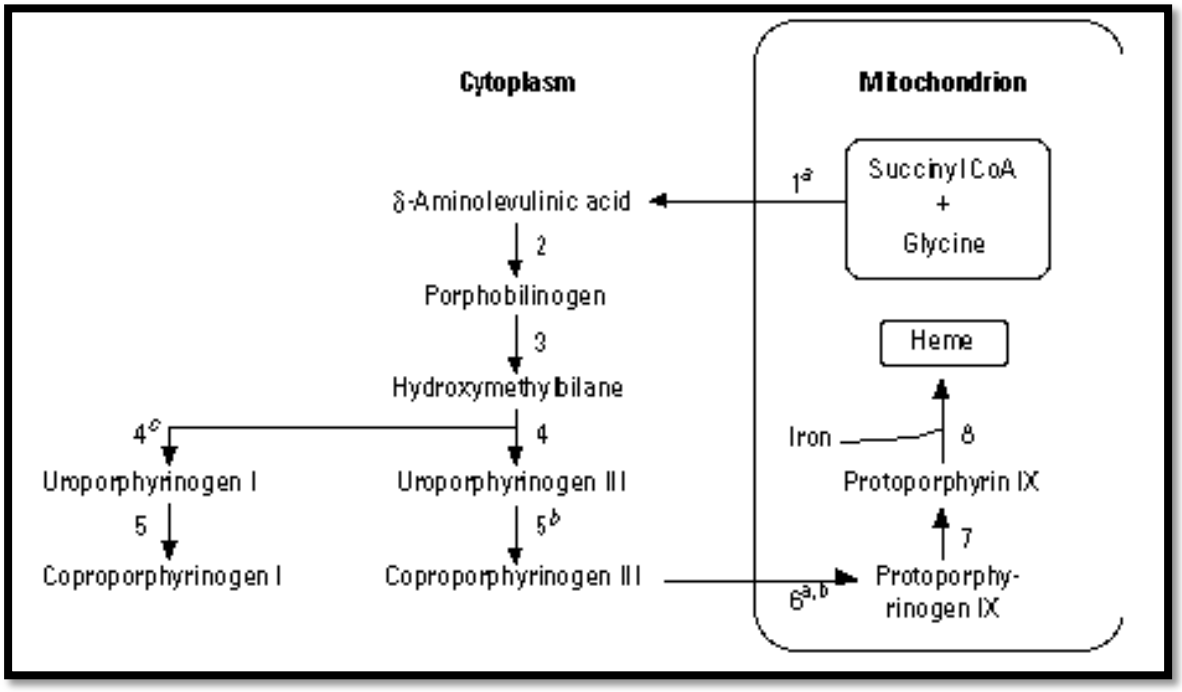

Figure 3. Heme Biosynthesis Pathway. Altered activity of ferrochelatase, an enzyme involved in hemoglobin synthesis (particularly the insertion of ferrous iron into protoporphyrin-IX), prevents the conversion of protoporphyrin-IX to heme (step 8) thus resulting in accumulation of Pp-IX in many tumor cells (Daniell et al., 1997).

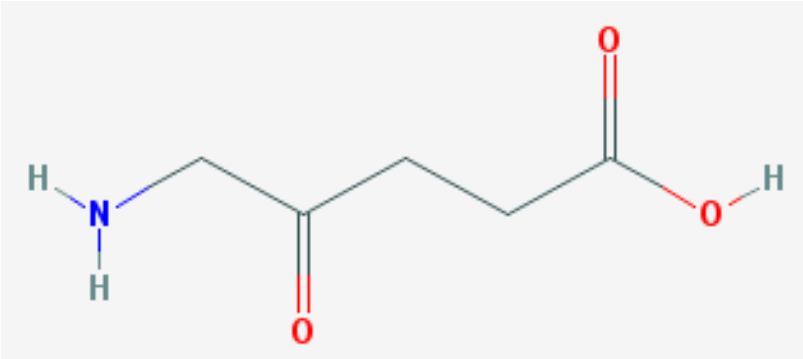

Figure 4. Molecular Structure of 5-Aminolevulinic Acid; MW = 131.13 g/mol

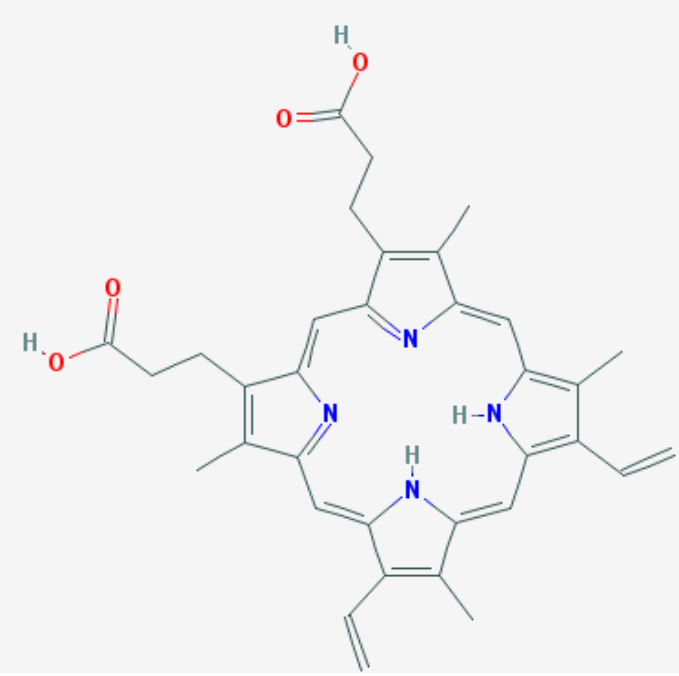

Figure 5. Molecular Structure of Protoporphyrin-IX; MW = 562.66 g/mol

Surgical microscopes currently being used for FGS have a relatively lower sensitivity and a higher cost when compared to SpectroPen. Though 5-ALA has improved the process of glioblastoma cell detection intraoperatively, the current, standard technology with operative microscopes could be improved upon as well, thereby making the process of glioblastoma resection by neurosurgeons even more efficient. SpectroPen would enable ultrasensitive detection of glioblastoma cells during resection, while

operating at a much lower cost (Mohs et al., 2010). Surgical microscopes operate at a long working distance, as much as 30 centimeters; the cumbersome device can be safely operated at a relatively larger distance away from the patient and the tissue than that of SpectroPen, which can be placed within a centimeter of the tumor cells. The benefit of having the source of irradiation close to the tissue can be understood by considering the inverse square law for light (Gates, 1980). The intensity of light decreases from a point source exponentially, with the square of the distance; this relationship is a result of the growing radius of the light wavefront as distance increases (Gates, 1980). Thus, being able to position SpectroPen in close proximity to tissue allows for the use of lower-power, less expensive light sources, increased fluorescence detection sensitivity (~1000x more sensitive) and enhanced fluorescence intensity on the corresponding spectra. Enhanced signal intensity is pivotal for detecting cells in the tumor margins, where fluorescence emission is notably less than that of the bulk tumor mass itself. Additionally, the ability to place the SpectroPen in close to tissue results in greater accuracy in detection of Pp-IX signal and in differentiation from background autofluorescence. Therefore, the longer working distance of surgical microscopes can lead to incorrect or incomplete delineation of tumor boundaries and cells in the margins (Mohs et al., 2010).

In order to test the hypothesis that SpectroPen is capable of ultrasensitive detection of tumor cell fluorescence, a threshold experiment will be performed in which the minimum number of fluorescent tumor cells detectable by the device will be recorded. Additionally, *in vitro* studies with a cancerous U87 EGFR vIII cell line as well as normal astrocytes and NIH/3T3 cell lines will be performed to test the hypothesis that

5-ALA's uptake and conversion to Pp-IX occurs preferentially in glioblastoma cells. *In vivo* studies in tumorigenic xenograft mice models will also be conducted.

Clinically, the intraoperative fluorescent-guided surgery would entail administering an oral dosage of exogenous 5-ALA (20 mg/kg body weight) approximately three hours before surgical intervention (Stummer et al., 2000). The contrast agent is non-toxic and is generally well-tolerated (Kennedy & Pottier, 1992).

METHODS

The 5-aminolevulinic acid and protoporphyrin-IX used throughout this project were purchased from Sigma-Aldrich. RPMI medium (1640, 1x) with 10% fetal bovine serum (FBS) and 5% penicillin streptomycin, along with phosphate buffered saline (with calcium and magnesium), was purchased from Corning for cell culture. Gill's Hematoxylin, Eosin Y salt, and Cryo-OCT Compound were purchased from Fisher. 2x Eosin Y stock was made by dissolving 5 grams of Eosin into 2.5 mL acetic acid and 500 mL 70% ethanol. Before staining, the 2x solution was diluted 1:1 with 70% ethanol. No additional modification or purification of these reagents was done. Animals: All experimental protocols strictly conformed to National Institutes of Health guidelines for the Care and Use of Laboratory Animals, and were approved by the Institutional Animal Care and Use Committees of Emory University.

SpectroPen Design and Setup

The SpectroPen was designed using a bifurcated fiber optic probe, connected to a 405 nm (violet) LED light source and a 16-bit spectrometer (Ocean Optics QE65000) (Figure 6). The SpectroPen probe is comprised of seven fibers in total: one fiber for

emission, or detection of fluorescence, surrounded by six excitation fibers that emit the violet light.

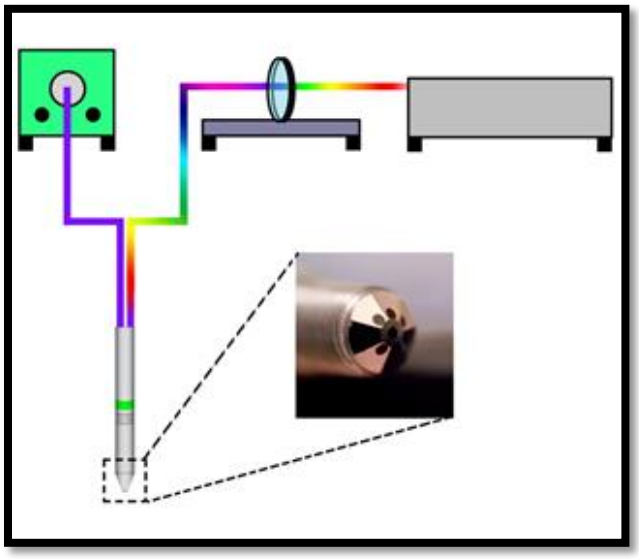

Figure 6 . Design and Setup of SpectroPen. SpectroPen consists of a bifurcated fiber optic probe attached to a LED light source and a spectrometer.

In Vitro Studies

The cell lines used in this project consisted of primary, normal human astrocytes, non-cancerous, NIH/3T3 mouse fibroblast cells, and U87 EGFR vIII glioblastoma cells (transfected with a plasmid for overexpressing the epidermal growth factor receptor vIII).

U87 EGFR vIII tumor cells were tested via fluorescent microscopy in 5-ALA staining studies to observe 5-ALA uptake and conversion to Pp-IX in tumor cells. 8-well LabTek chamber slides were coated with Poly-L-Lysine for ~one hour before the Poly-Lysine was removed and the wells allowed to air-dry; this was done to facilitate cell adhesion to the glass-bottomed wells of the chamber slide through the addition of a thin, positively-charged coating. The U87 EGFR vIII tumor cells were plated in the wells and cultured at 37°C and 5% CO_2. Once 60% confluent, the tumor cells were incubated with 5-ALA (2mM) for ~24 hours before being washed with 1x PBS and imaged under a

fluorescent microscope (Olympus IX71, 488 nm excitation and long-pass filter for emission). The images were subsequently analyzed with ImageJ and Nuance software to confirm the presence of Pp-IX fluorescence in the tumor cells; the presence of Pp-IX fluorescence resulted in characteristic, protoporphyrin-IX spectral peaks at ~635 nm and ~704 nm.

Astrocytes and NIH/3T3 cells were treated with a similar protocol for imaging. The astrocytes and NIH/3T3 cells were the negative control against which the tumor cells were measured, as these normal cells should display no fluorescent emission. These non-tumorigenic cells were cultured at 37°C and 5% CO_2 to approximately 50%, as the cells appeared to change morphology when allowed to grow to higher confluency. As with the staining treatment for U87 EGFR vIII cells, both normal cell lines were incubated with 5-ALA (2mM) for ~24 hours before being washed with 1x PBS and imaged under a fluorescent microscope (Olympus IX71, 488 nm excitation and long-pass filter for emission). The images were analyzed using ImageJ and Nuance software, to verify the lack of Pp-IX fluorescence.

SpectroPen Sensitivity Experiment

To test for SpectroPen sensitivity, or the threshold cell count for SpectroPen detection of fluorescence emission from tumor cells, U87 EGFR vIII cells were cultured in a T-25 flask at 37°C and 5% CO_2 to 80% confluency and treated with 2mM 5-ALA ~24 hours before being washed with 1x PBS and harvested with 0.05% trypsin. The cells were then resuspended in 2 mL of growth medium in a 15 mL conical tube, and the cell solution was spun down at 1,500 RPM for 4 minutes in a centrifuge. The supernatant

(growth medium) was aspirated and the cells resuspended in 2 mL of 1x PBS for counting with a hemacytometer. 10 µL of the cell solution was pipetted onto the hemacytometer counting chamber to determine the concentration of the cell solution, from which the appropriate dilution calculations were performed to determine the volume of cell solution to add for each value (cell number) being tested: 0; 1,000; 2,500; 5,000; 10,000; 20,000 and 50,000 cells; three replicates for each cell sample was tested. Each value of cells was added to 1.5 mL microcentrifuge tubes, and each tube was filled to a total volume of 500 µL with 1x PBS. All the microcentrifuge tubes were spun down in a microcentrifuge set to 4,000 RPM for 4 minutes, in order to concentrate the cells for fluorescence measurement. The tubes were then analyzed using the SpectroPen and spectral software. The cell pellets in each tube were irradiated with violet, 405 nm light from the SpectroPen, and the corresponding spectra were recorded and saved for intensity analysis.

To analyze the data, fluorescence intensity of the spectra, or height of the emission peaks, was quantified by calculating the integral, or area under the curve, for the characteristic range of protoporphyrin-IX fluorescence. Here, the integral was taken under the 600-725 nm wavelength range, as the Pp-IX emission spectrum rises, peaks, and falls within this window. The mean of the integral for the replicates of each cell number (a proxy for fluorescence intensity of each cell number) was plotted against the number of cells in the sample. Standard deviation of the integrals for the replicates was calculated for each cell number, and included in the graph.

In Vivo Mice Trials

Nude, immunocompromised (athymic) mice 6-8 weeks old were injected with U87 EFGR vIII tumor cells in the right cerebral hemisphere 14 days before the brains were tested with SpectroPen. A T2 MRI was taken seven days after implantation, and on the day of imaging, the mice were administered 5-ALA (200mg/kg body weight) orally or intraperitoneally approximately two hours before testing for fluorescence in the tumor. Immediately following protoporphyrin-IX tumor cell fluorescence testing with SpectroPen, the mice brain tissues were embedded with OCT gel, frozen, and cryosectioned for histologic analyses in order to verify that the fluorescence signal detected corresponded to the tumor mass in the brain. Coronal sections of the brains were prepared, and a hematoxylin and eosin stain was performed to visualize the presence of the glioblastoma tumor tissue. Lastly, fluorescence imaging of the brain sections was done to confirm the *in vivo* specificity of the Pp-IX accumulation to the tumor cells.

Fluorescein and Protoporphyrin-IX Mixtures: Spectral Distinction Experiment

In order to distinguish between the fluorescence emission peaks of fluorescein and Pp-IX upon simultaneous excitation of the contrast agents, tests were performed with the two dyes to determine the efficacy of spectral identification using software. This test was performed as a preliminary measure for future studies involving the simultaneous administration of protoporphyrin-IX and fluorescein to immunocompromised mice, as part of a comparison study between the efficacies of the two agents for tumor localization and specificity. The premise of the study was to observe whether the emission peaks of the two dyes could be simultaneously recorded and distinguished on a single fluorescence

emission spectrum, using 405 nm excitation from the SpectroPen. Despite the excitation of fluorescein and protoporphyrin-IX differing- fluorescein's is about 500 nm whereas protoporphyrin-IX's is ~400 nm- the 405 nm excitation was sufficiently apt for excitation of both dyes. Different ratios of Pp-IX and fluorescein were made up in glass vials; it should be noted, in this case, that protoporphyrin-IX solution was made instead of 5-ALA solution, as the study did not rely upon tumor cells' selective uptake and conversion of 5-ALA to Pp-IX. Rather, it aimed to compare innately fluorescent agents in solutions comprised of different ratios of each dye. 1 mM (arbitrarily chosen concentration) of protoporphyrin-IX was dissolved in 5 mL of DMSO, and the working concentration of fluorescein, which was dissolved in DI H_2O, was 10 µM (100x more dilute than Pp-IX) to account for its relatively more robust fluorescence. The fluorescence emission peaks were normalized such that the peak intensities on the spectrum of the two stock solutions were approximately the same. This allowed for a level, balanced fluorescence intensity from both contrast agents to start, so that emission peak heights from each mixture would better correspond with concentration of each contrast agent relative to the other. The ratios of contrast agents included 75:25, 90:10, 95:5, 100:0 for fluorescein to Pp-IX as well as for Pp-IX to fluorescein; eight mixture solutions in total.

Each vial was then irradiated with 405 nm violet light from the SpectroPen, and the corresponding peaks were recorded. Theoretically, the intensity of the peaks should have tracked with the ratio of the respective dye, for instance, a vial with 95% Pp-IX was expected to display a more intense peak than a vial with a lower ratio of Pp-IX, such as 75% Pp-IX. A software program was employed, Microsoft Excel in this case, for analysis

of the spectra and to ensure that a clear distinction of the two fluorescent agents could be made.

Least squares fitting was used to quantify the difference between the experimentally-acquired values of fluorescence intensity/mixture ratio, calculated by the software algorithm, and the expected values of fluorescence intensity/mixture ratio (0.95, 0.90, and 0.75) set for each dye. This mathematical procedure involves minimizing the sum of the squares of the residuals of the points, the data values in this case, from the known curve, or the expected fluorescence intensity values/mixture composition (Weisstein, 2014). The actual values of fluorescence intensity were derived via an algorithm that calculated these numbers from the experimental data, given the fluorescence intensity of the pure, 100% sample of each contrast agent. Therefore, using the 100%, pure samples of each dye as a control, the experimental values of fluorescence intensity for each mixture was scaled relative to the pure sample. These calculated, scaled values indicated the actual composition of each mixture; they were then compared to the expected concentration values for each mixture. The resulting ratios of actual to expected values allowed for a quantification of how well the fluorescence intensities of the spectral peaks for each dye tracked with the intended intensities.

RESULTS AND DISCUSSION

The results of this study show that uptake of 5-ALA and conversion to Pp-IX occurs preferentially in tumor cells, in the U87 EGFR vIII_cell line, as fluorescence emission from Pp-IX is detected in these glioblastoma cells. The spectra for these tumor cells displays characteristic protoporphyrin-IX peaks (Figure 7C), whereas that for the

normal cell lines tested, astrocytes and NIH/3T3, show no such emission peaks and fluorescence intensity (Figure 8B, Figure 9B). Using the metabolic contrast agent in conjunction with the SpectroPen has proven that this technology can be used to accurately identify U87 EGFR vIII cells *in vitro*, with a signal to noise ratio of 100:1, and to detect fluorescence from as few as 2,500 tumor cells (Figure 10). The data indicate that both hypotheses tested cannot be rejected.

A) 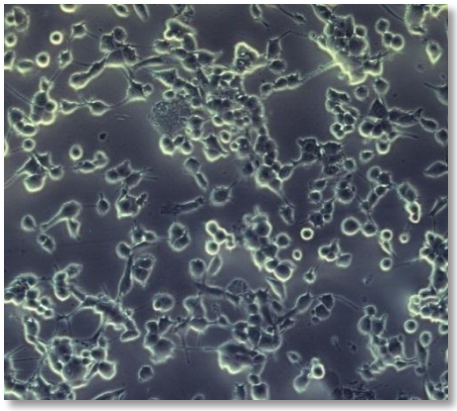

B) 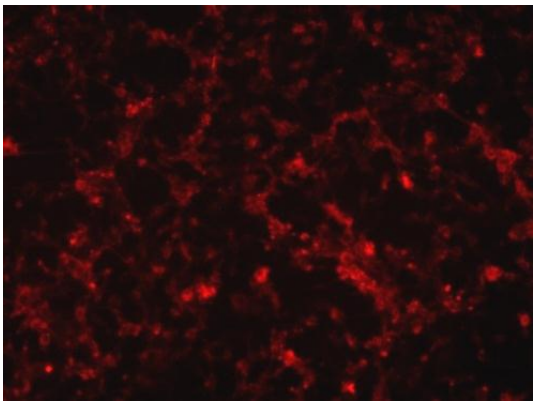

C) 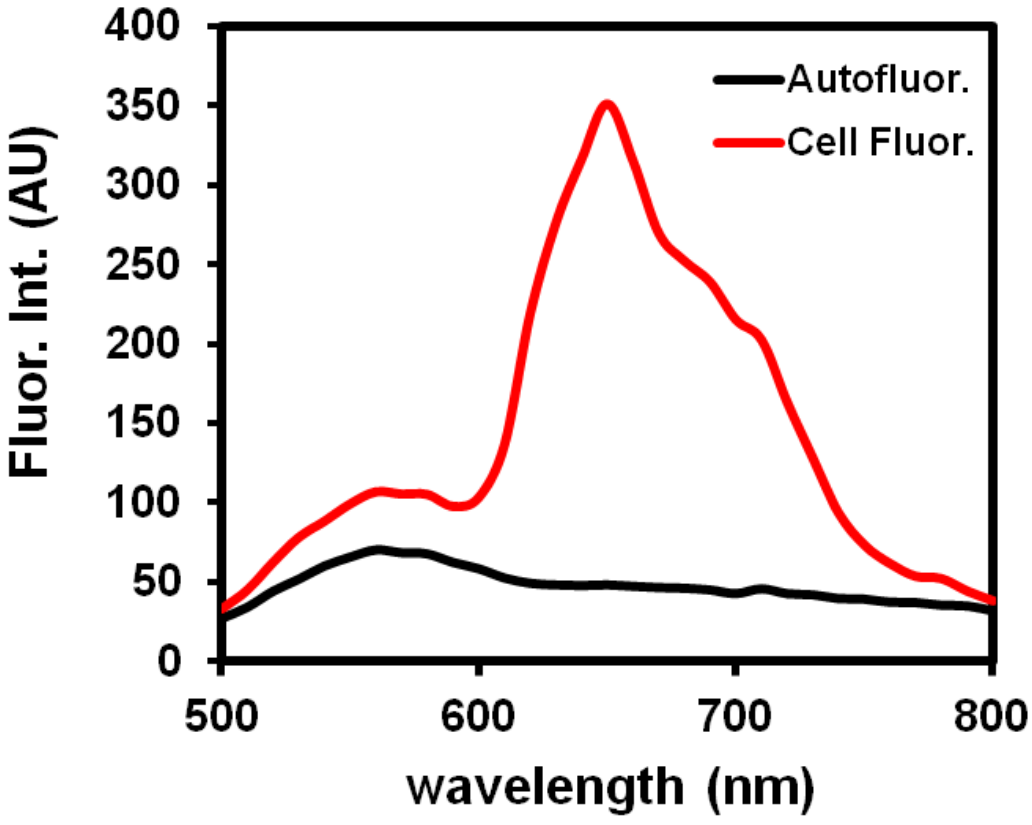

Figure 7. *In Vitro* Study of Uptake and Conversion of 5-ALA to Pp-IX in U87 EGFR vIII Tumor Cells. **A.** Bright-field image of U87 EGFR vIII cells. **B.** Corresponding fluorescence image, showing red fluorescence of Pp-IX. **C.** Spectrum obtained from the fluorescence image shows the characteristic Pp-IX peaks at ~635 nm and ~704 nm.

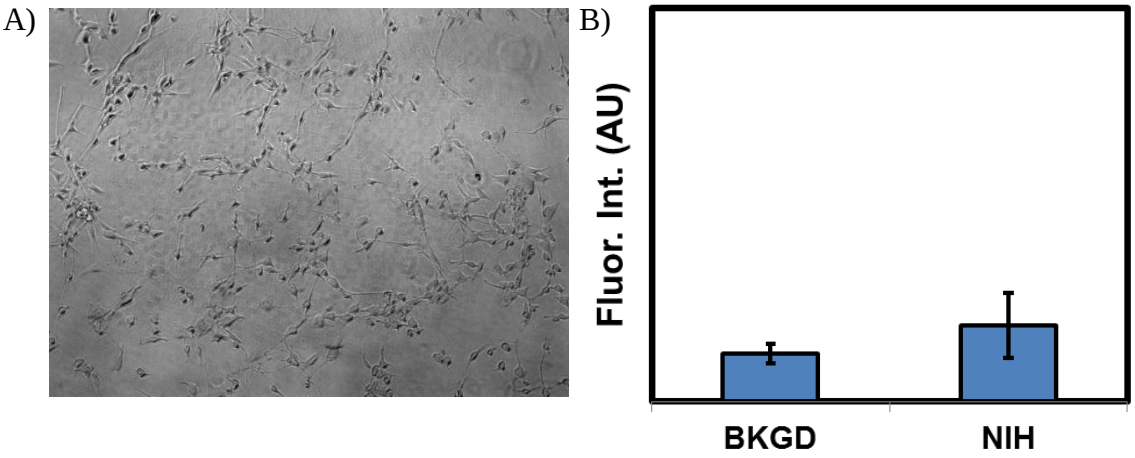

Figure 8. *In Vitro* Study of Uptake and Conversion of 5-ALA to Pp-IX in Normal, Mouse Fibroblast Cells, NIH/3T3. **A.** NIH/3T3, normal mouse fibroblast cells show no fluorescent emission from Pp-IX. **B.** Normal cells show minimal fluorescence signal, which is not statistically distinct from background fluorescence.

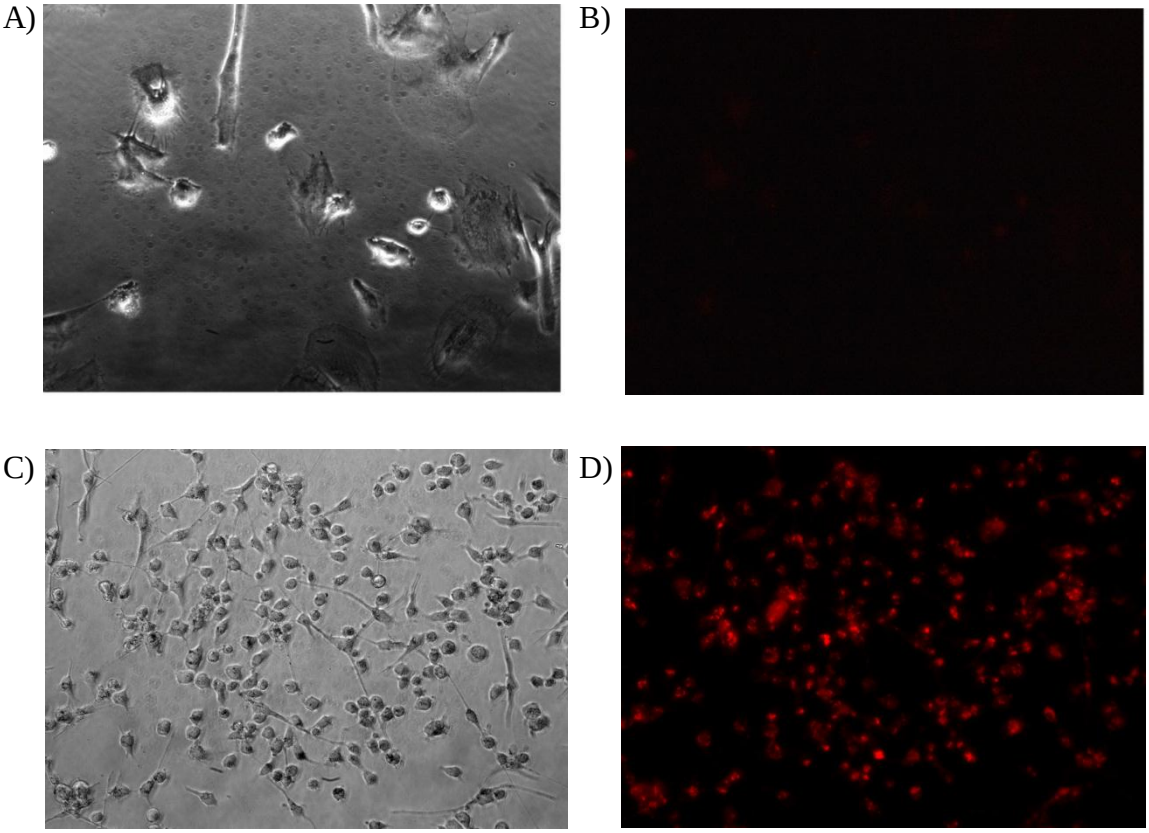

Figure 9. *In Vitro* Comparative Studies of Uptake and Conversion of 5-ALA to Pp-IX in Normal, NIH/3T3 Cells and U87 EGFR vIII Tumor Cells. **A.** Bright-field image of normal human astrocytes. **B.** After incubation with 5-ALA, there is no evidence of protoporphyrin-IX accumulation in the cells as evident by the lack of fluorescence emission. **C.** Bright-field image of U87 EGFR vIII cells. **D.** Following incubation with 5-ALA, there is red fluorescence signal detected from the protoporphyrin-IX buildup in the tumor cells.

FGS using SpectroPen operates by detecting fluorescence emission of endogenous Pp-IX, a metabolite of 5-ALA that the tumor cells accumulate in higher concentrations upon administration of exogenous 5-ALA (due to malignant cell deficiencies in ferrochelatase (Figure 3), an enzyme that functions in the production of heme from protoporphyrin-IX (Rubino et al., 1966), as well as enhancement of deaminase activity (Navone et al., 1991)).

The likelihood of false positives, given by normal tissue fluorescence, is reduced by using 5-ALA as a contrast agent. Significant fluorescence as a result of 5-ALA conversion to Pp-IX is observed in cells with particular defects in the heme biosynthesis pathway that result in the accumulation of the fluorescent Pp-IX, as opposed to normal cells that have no defects in the pathway and thus no fluorescence emission (Figure 9). This is in contrast to the uptake mechanisms of other contrast agents that rely upon tumor localization due to tumors' rapid neovascularization and the enhanced permeability and retention effect (EPR). Such dyes include the constantly-fluorescent ICG (Kosaka et al., 2011) and fluorescein (Cho et al., 2008; Singh et al., 2012) , which have a relatively higher probability for false positives if localized in normal tissue- because of their constant fluorescence (Huang et al., 2010).

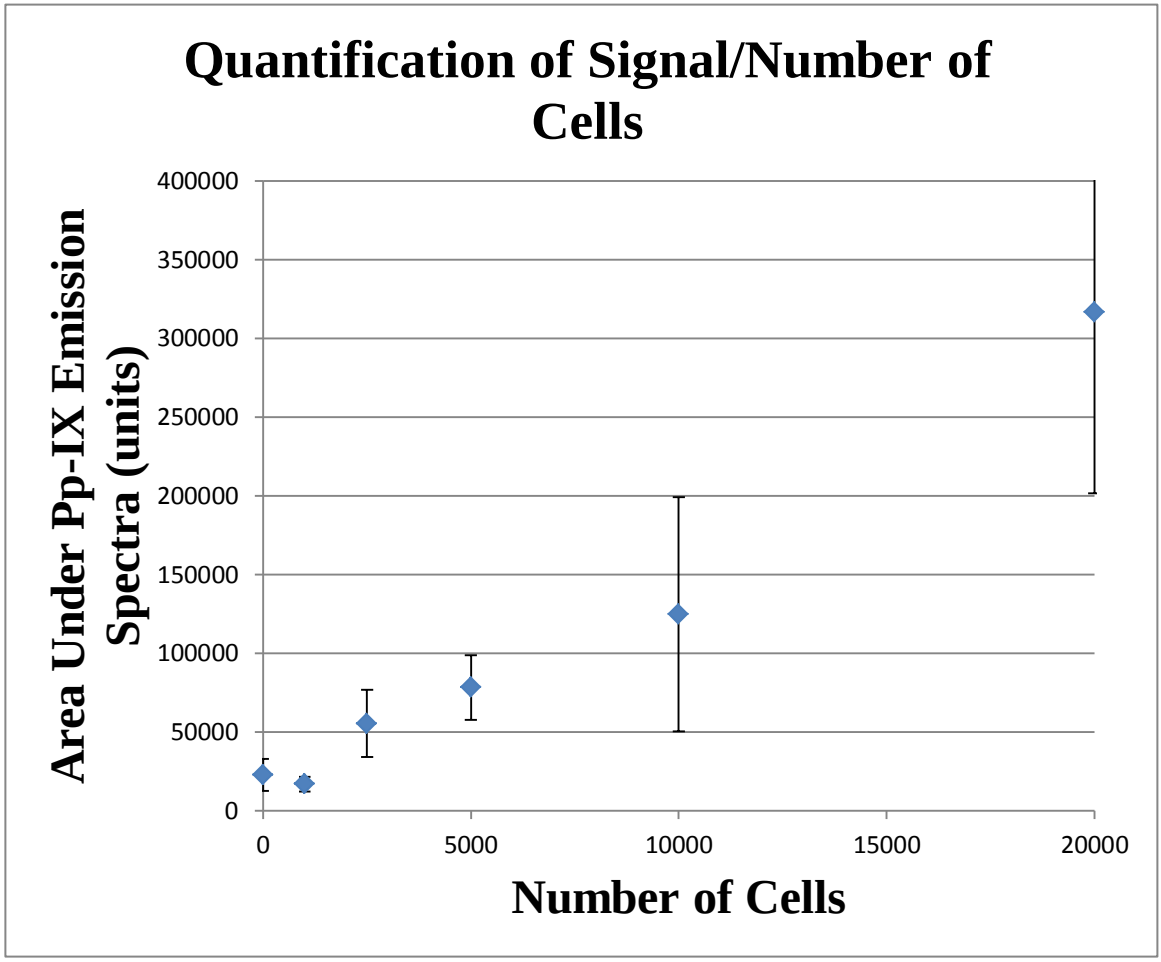

Figure 10. SpectroPen Sensitivity Study: Minimum Number of Tumor Cells with Detectable Fluorescence Emission. Relationship between the number of U87 EGFR vIII cells exhibiting fluorescence and the area under the peak for the 600-725 nm wavelengths, or the fluorescence emission intensity of protoporphyrin-IX. The SpectroPen detects the greatest fluorescence intensity for the 20,000 cells sample (50,000 cell sample not shown on plot; significantly greater fluorescence intensity) but is also sensitive enough to pick up fluorescence with a sample as little as 2,500 cells.

In vivo studies with mice brains confirm the efficacy of this technology in organisms, and verify the results seen in the *in vitro* experiments. Upon irradiation with 405 nm light, mice- previously administered 5-ALA- show characteristic Pp-IX fluorescence specific to the implanted tumor in the right hemisphere of the brains (Figures 11B, 12B, 13B). The bulk tumor mass exhibited robust fluorescence from Pp-IX, and the surrounding tumor margins had weaker fluorescence due to the relatively

fewer number of tumor cells present. SpectroPen, with its mobility that allows surgeons to place the device within a centimeter of the tissue of interest, allows maximal detection sensitivity in such margins, where fluorescence is less than that observed in the bulk tumor mass. This is in contrast to surgical microscopes, which cannot be placed as close to the tissue of interest and, as a result of the inverse square law for light, are less sensitive to fluorescence in the diffuse tumor margins. Irradiating the left hemispheres with 405 nm showed no fluorescence emission, as this region did not have any tumor cells implanted and was assumed to be comprised of only normal brain cells. MRI images confirm the location of the tumor masses as being only in the right hemispheres, and corroborate the data collected from the fluorescence studies (Figure 11C). The coronal sections of the mice brains and subsequent hematoxylin and eosin staining also confirm the location of the tumor cells in the right hemispheres of the brains, as the tumor mass stained blue while the normal cells surrounding the bulk tumor stained lighter purple (Figure 11D).

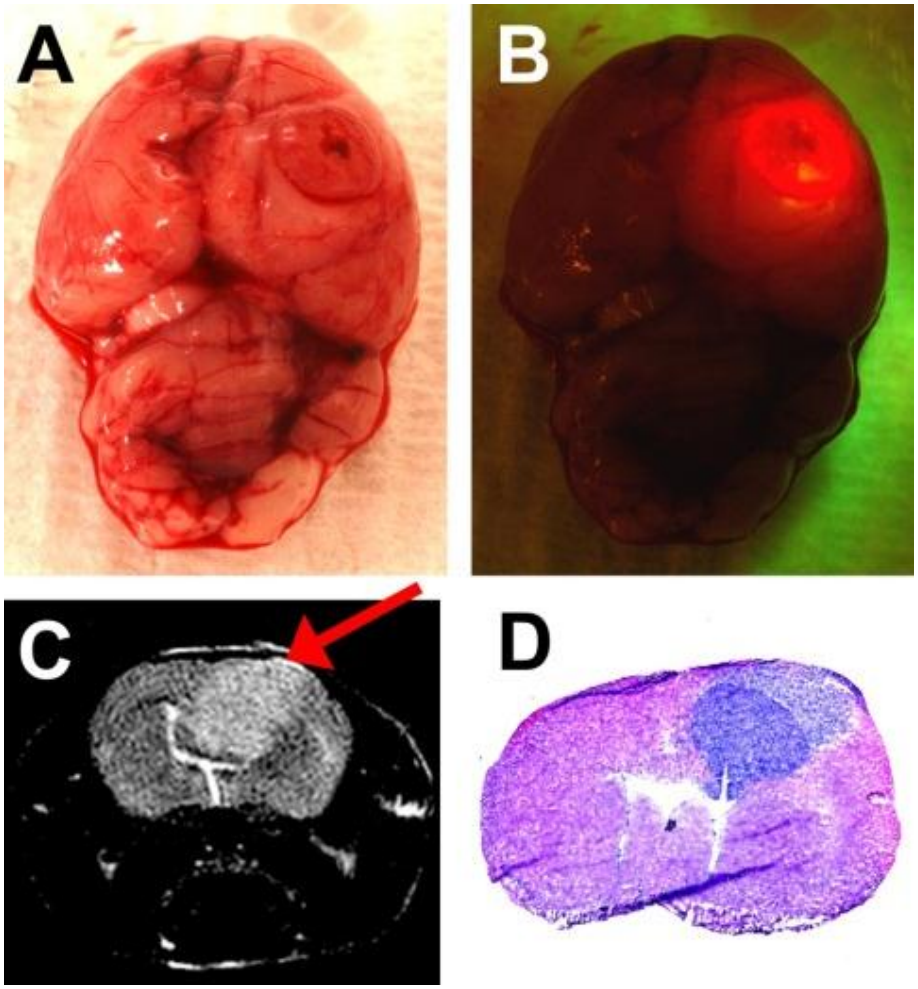

Figure 11. *In Vivo* Study of 5-ALA Uptake and Conversion to Pp-IX in Implanted Tumors. Intracranial glioblastoma xenograft mouse model for *in vivo* studies. **A.** Color photograph of the mouse brain 14 days after U87 EGFR vIII tumor cells implantation. **B.** Fluorescence photograph of the mouse brain 2 hours after 5-ALA administration. Bright protoporphyrin-IX fluorescence is visible from the bulk tumor upon excitation with the SpectroPen. **C.** Tumor localization was verified with MRI prior to surgery **D.** Coronal histological sections immediately following spectroscopic investigations; the darker blue stain is the bulk tumor, as confirmed with MRI, data from the Pp-IX spectra, and fluorescence imaging.

A) B)

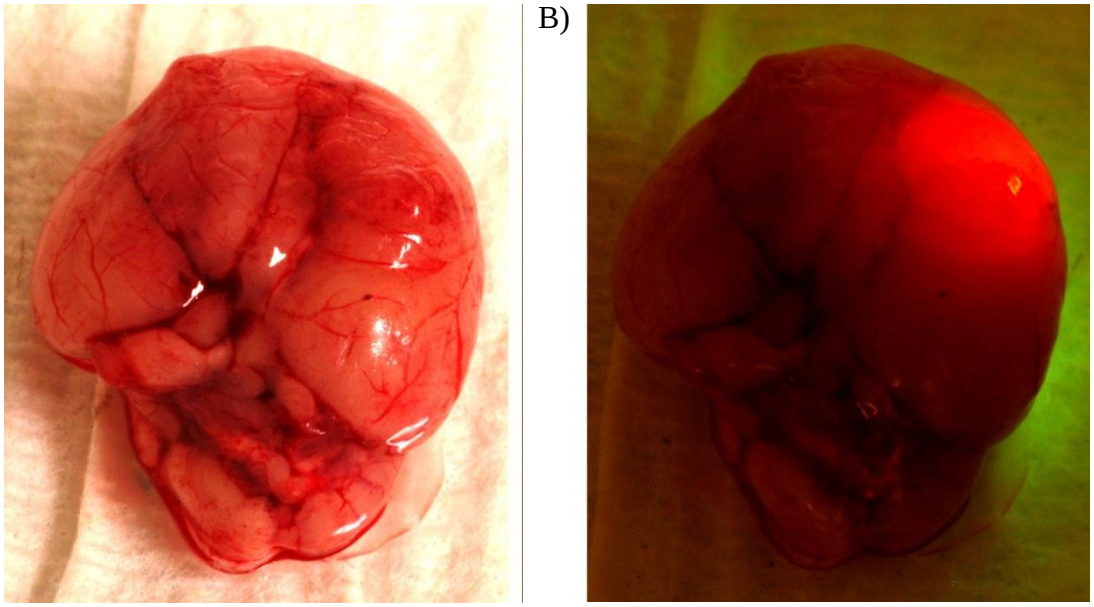

Figure 12. *In Vivo* Study of Tumor-Specific Pp-IX Fluorescence in Xenograft Model. Intracranial glioblastoma xenograft mouse model 2 for *in vivo* studies. **A.** Color photo of mouse brain 14 days after U87 EGFR vIII tumor cells implantation. **B.** Fluorescence photograph of the mouse brain 2 hours after 5-ALA administration. Bright Pp-IX fluorescence is visible from the bulk tumor upon excitation with the SpectroPen.

A) B)

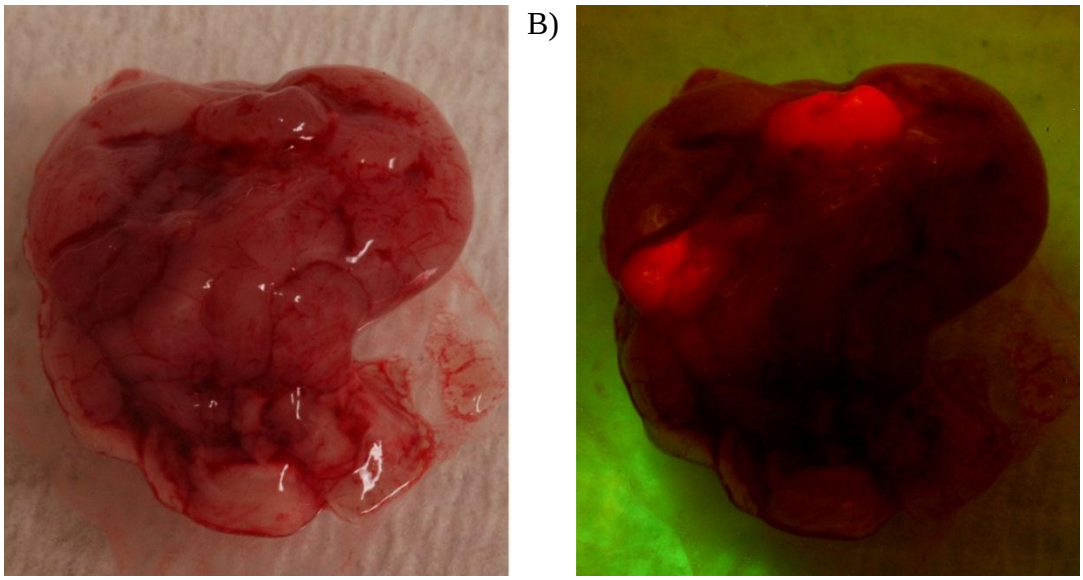

Figure 13. *In Vivo* Study of Tumor-Specific Pp-IX Fluorescence in Xenograft Model. Intracranial glioblastoma xenograft mouse model 3 for *in vivo* studies. **A.** Color photo of mouse brain 14 days after U87 EGFR vIII tumor cells implantation. **B.** Fluorescence photograph of the mouse brain 2 hours after 5-ALA administration. Bright protoporphyrin-IX fluorescence is visible from the bulk tumor upon excitation with the SpectroPen.

To test for tumor specificity and sensitivity between the FDA-approved contrast agent, fluorescein, and 5-ALA, currently not FDA-approved, a direct comparison study within a single organism is necessary. Such an experiment would involve the co-administration of both contrast agents in an organism, to avoid variation that arises from administration in different organisms, and simultaneous excitation of both dyes to observe for the dye that has greater accumulation in tumor tissue. However, before this experiment can be performed, it is necessary to examine whether the emission signals can be differentiated on a single spectrum. In order to test for the ability to separate and distinguish the fluorescence emission peaks of two contrast agents, protoporphyrin-IX and fluorescein, on a single spectrum, mixtures of the two dyes in varying concentrations were made. A software algorithm was used to separate the signals, as both dyes within the mixture were simultaneously irradiated with 405 nm light, and to determine the relative concentrations of each contrast agent in the various mixtures. These relative concentrations of contrast agent, calculated by the algorithm, were then compared to the expected concentrations used to make up each mixture. This study was done as preliminary measure, to enable future studies *in vivo* that would allow for quantification of contrast agent localization at a particular tumor site. A direct comparison between fluorescein and Pp-IX could be made, and the relative intensities of the emission peaks would be a good indicator of which dye had greater accumulation at the site of the tumor.

This study demonstrates that the fluorescence emission peaks of each can be plotted on one spectrum and differentiated using least squares fitting (Figure 14). This experiment confirms the efficacy of simultaneously measuring fluorescence emission of two dyes, and of being able to observe emission peaks that correspond to the relative

concentration of the dye present. The experimental data closely resemble the expected results, as evidenced by the ratios of actual values to expected values being near one (Table 1).

Table 1. Ratio of Actual/Expected Signal Intensity. The ratio of experimentally-determined, or actual, fluorescence intensity to the expected fluorescence intensity, calculated from the software algorithm, indicates the proximity in values for each concentration of contrast agent. The ratios are close to 1:1 for both dyes at each concentration. When the signals are viewed on the spectrum, there is substantial overlap between the actual and expected peaks (Figure 14B-D, F-H).

Ratio of Actual/Expected Signal Intensity		
	Contrast Agent	
Mixture (% of Pure Sample)	Protoporphyrin-IX	Fluorescein
0.95%	0.96	1.02
0.90%	0.97	1.03
0.75%	1.11	0.99

*Working concentration of Pp-IX = 1 mM

*Working concentration of fluorescein = 10 µM

A)

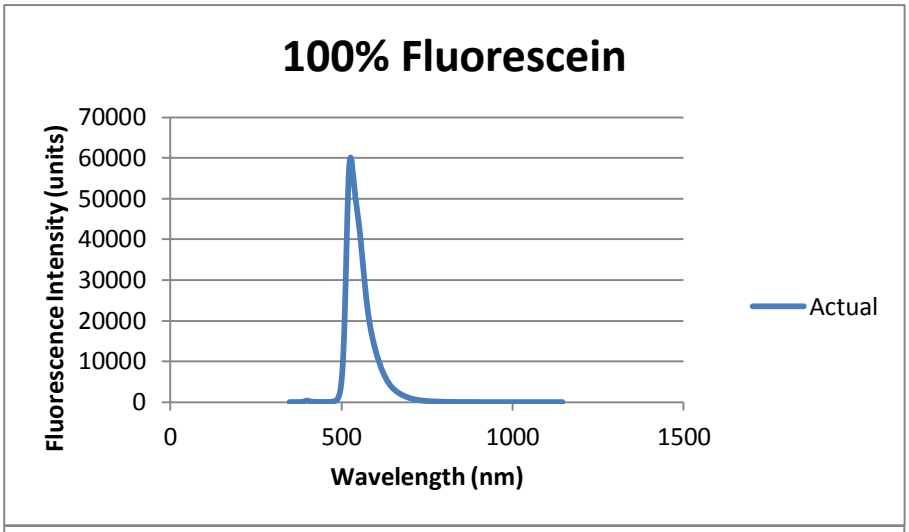
100% Fluorescein
Fluorescence Intensity (units)
70000
60000
50000
40000
30000
20000
10000
0
0
500
1000
1500
Wavelength (nm)
Actual

B)

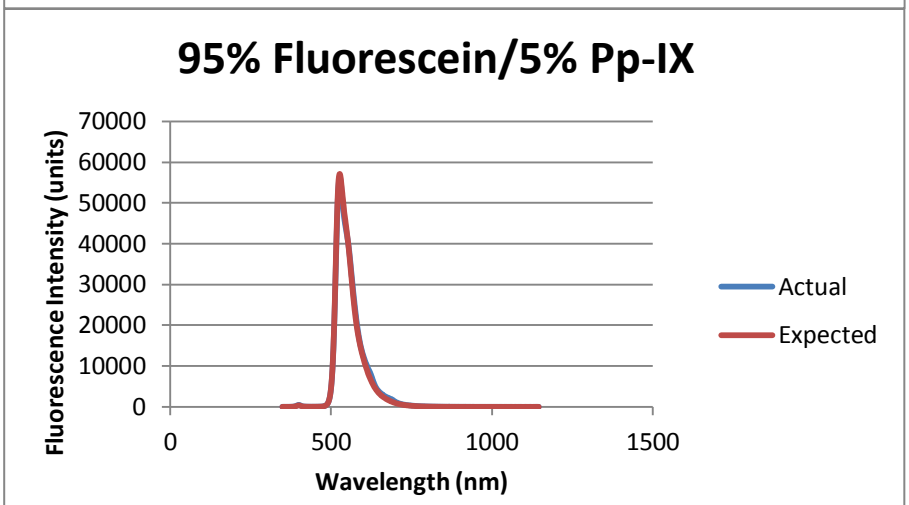
95% Fluorescein/5% Pp-IX
Fluorescence Intensity (units)
70000
60000
50000
40000
30000
20000
10000
0
0
500
1000
1500
Wavelength (nm)
Actual
Expected

C)

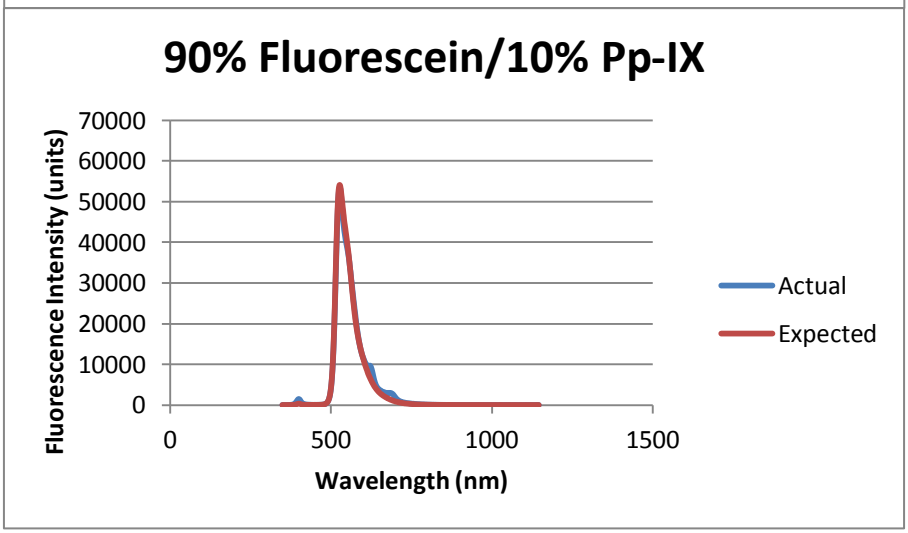
90% Fluorescein/10% Pp-IX
Fluorescence Intensity (units)
70000
60000
50000
40000
30000
20000
10000
0
0
500
1000
1500
Wavelength (nm)
Actual
Expected

D)

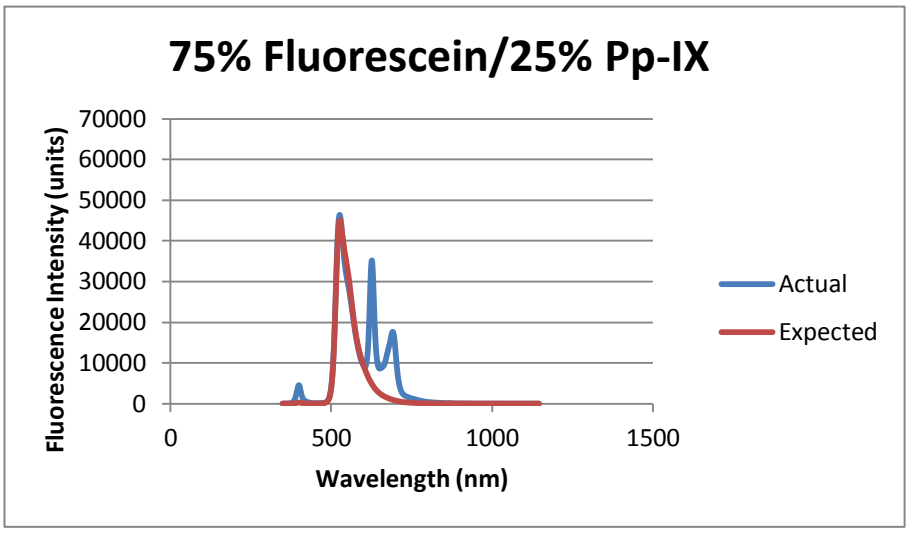
75% Fluorescein/25% Pp-IX
Fluorescence Intensity (units)
70000
60000
50000
40000
30000
20000
10000
0
0
500
1000
1500
Wavelength (nm)
Actual
Expected

E)

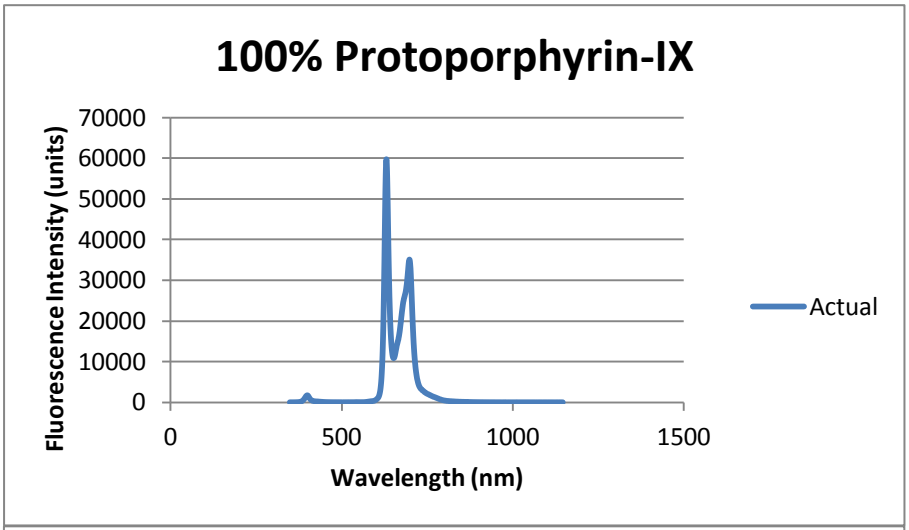
100% Protoporphyrin-IX
Fluorescence Intensity (units)
70000
60000
50000
40000
30000
20000
10000
0
0
500
1000
1500
Wavelength (nm)
Actual

F)

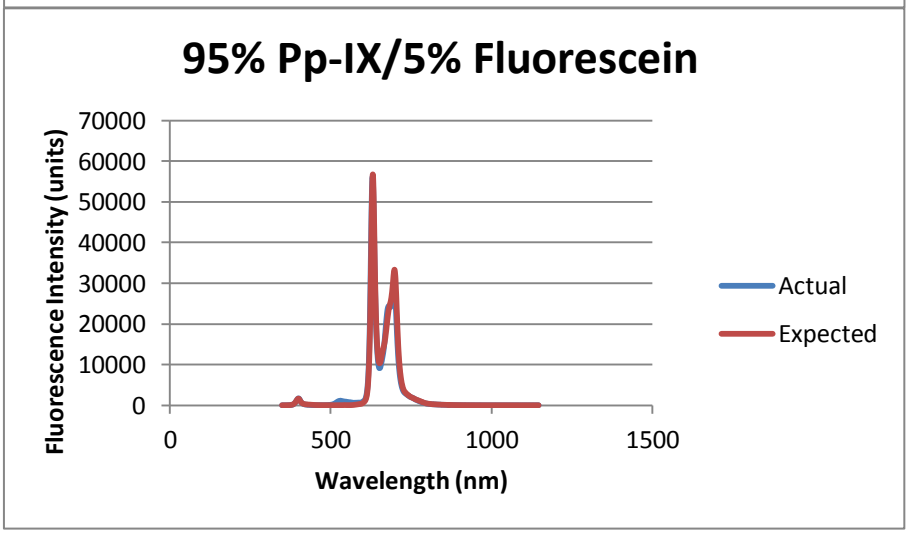
95% Pp-IX/5% Fluorescein
Fluorescence Intensity (units)
70000
60000
50000
40000
30000
20000
10000
0
0
500
1000
1500
Wavelength (nm)
Actual
Expected

G)

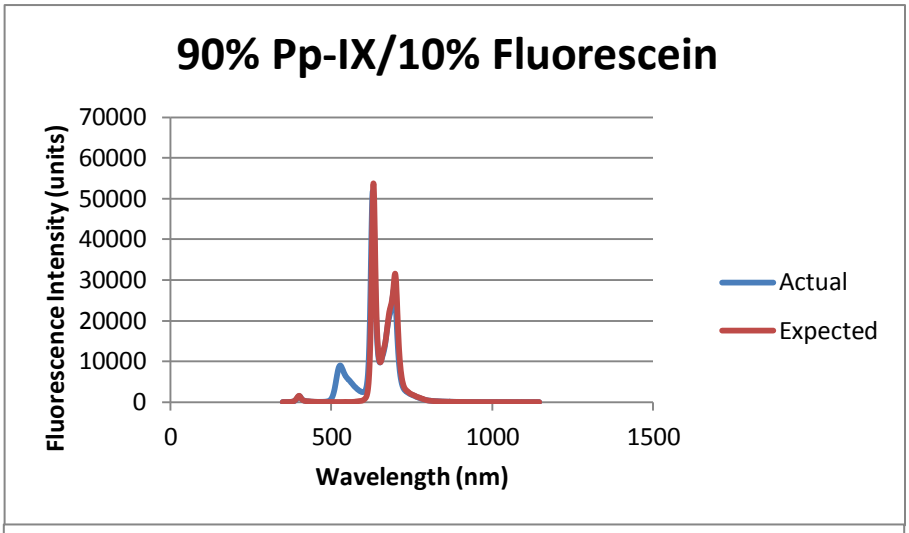

H)

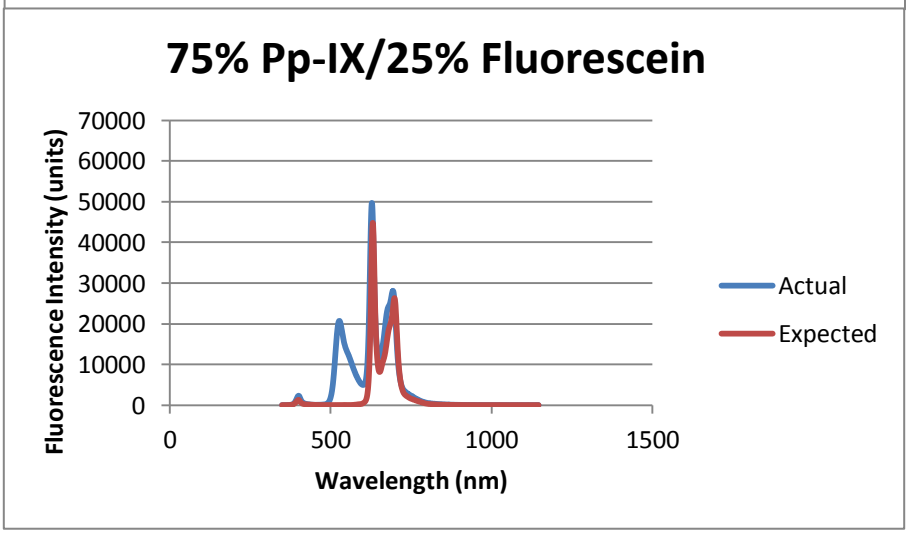

Figure 14. Fluorescence Emission Spectra for Fluorescein and Pp-IX Mixtures. **A.** Spectrum for 100% pure fluorescein displays its characteristic peak at ~500 nm and a maximum intensity of ~60,000 units. **B.** Spectrum for mixture containing 95% fluorescein and 5% Pp-IX shows close correlation to predicted fluorescence intensities and lower maximum intensity relative to pure sample. **C.** Spectrum for mixture containing 90% fluorescein and 10% Pp-IX shows close correlation to predicted fluorescence intensities and lower maximum intensity relative to 95% sample. **D.** Spectrum for mixture containing 75% fluorescein and 25% Pp-IX shows close correlation to predicted fluorescence intensities and lower maximum intensity relative to 90% sample. **E.** Spectrum for 100% pure Pp-IX displays its characteristics peaks at 635 nm and 704 nm and a maximum intensity of ~60,000 units. **F.** Spectrum for mixture containing 95% Pp-IX and 5% fluorescein shows close correlation to predicted fluorescence intensities and lower maximum intensity relative to pure sample. **G.** Spectrum for mixture containing 90% Pp-IX and 10% fluorescein shows close correlation

to predicted fluorescence intensities and lower maximum intensity relative to 95% sample. **H.** Spectrum for mixture containing 75% Pp-IX and 25% fluorescein shows close correlation to predicted fluorescence intensities and lower maximum intensity relative to 90% sample.

The fluorescein and Pp-IX mixture study is a first step for future, *in vivo* experiments involving simultaneous administration of both dyes to test for specificity of accumulation in tumor tissue. The results indicate good accuracy of fluorescence intensity between the experimental values calculated by the algorithm and the expected concentrations of 0.95, 0.90, and 0.75. In subsequent studies, software analysis using the algorithm will be used to determine the distinction of the emission peaks from both contrast agents *in vivo* and to determine the amount of each fluorescent agent that has localized within animal tumor tissue. This procedure will involve co-administration of fluorescein and 5-ALA in xenograft mice models to examine the *in vivo* efficacies of fluorescein and 5-ALA in a direct comparison study. Both contrast agents will be simultaneously administered to the mouse, and their respective fluorescence intensities will be measured and compared, in addition to accumulation in RES organs, to test for tumor localization and specificity. Based on the data from the preliminary study of the dye mixtures, both contrast agents' fluorescence emission peaks should be able to be simultaneously characterized and distinguished on a spectrum in real-time. This study should show a clear advantage in using 5-ALA over fluorescein, in that there should be more tumor cell specificity and higher fluorescence intensity detected from protoporphyrin-IX rather than fluorescein, which should display off-target accumulation in reticuloendothelial organs.

Additionally, the scope of this experiment will be expanded to different tumor cell lines to test and to observe for similar results to those of glioblastoma cells. Breast cancer

cell lines such as ZR-75-1 (estrogen receptor positive) and 4T1 have been preliminarily tested, with many more tumorigenic cells including ovarian cancer, head and neck cancer, pancreatic, liver, and cervical cancer among others to be investigated.

A) 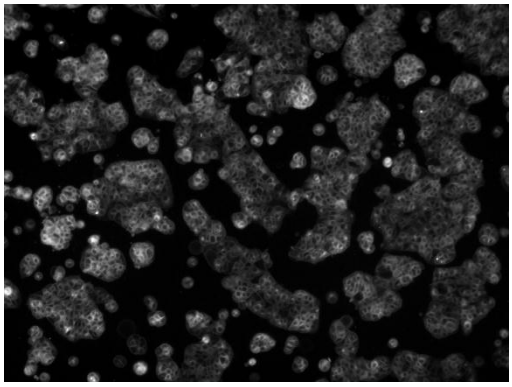 B) 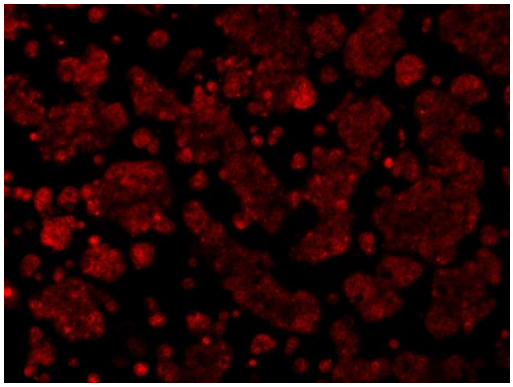

Figure 15. *In Vitro* Study of Uptake and Conversion of 5-ALA to Pp-IX in ZR-75-1 Breast Cancer Cells. **A.** Bright-field image of ZR-75-1 breast cancer cells. **B.** Following incubation with 5-ALA, there is red fluorescence signal detected from the protoporphyrin-IX buildup in the tumor cells.

A) 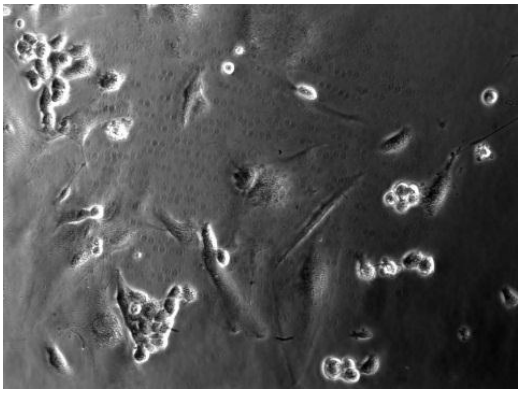 B) 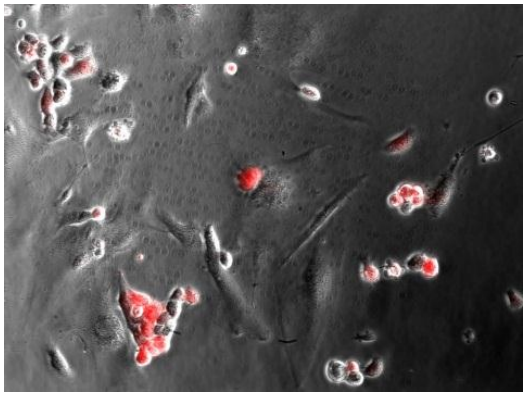

Figure 16. *In Vitro* Study of Specificity, Uptake and Conversion of 5-ALA to Pp-IX in Co-Culture of ZR-75-1 Tumor Cells and Astrocytes. **A.** Co-culture of astrocytes and ZR-75-1 breast cancer cells. **B.** Fluorescent imaging indicates that there is selective uptake and fluorescence emission in tumorous ZR-75-1 cells only.

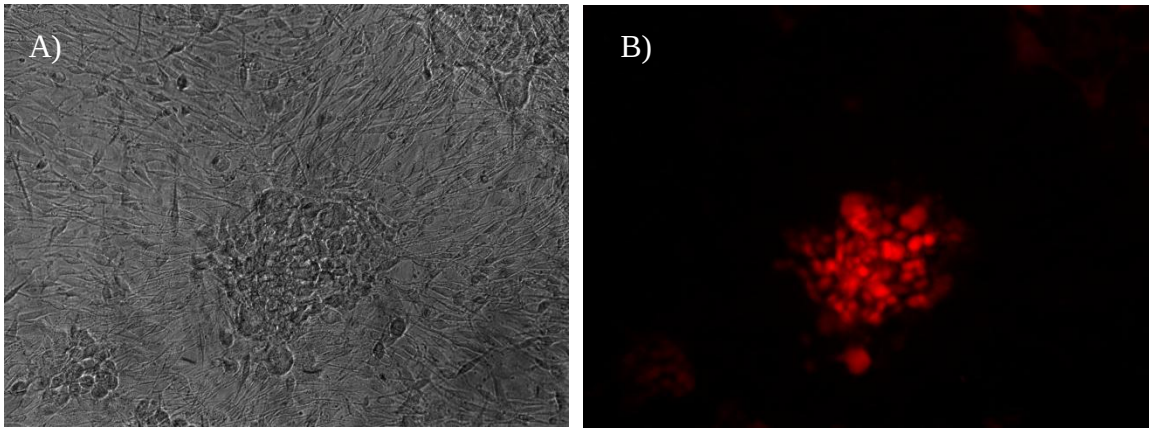

Figure 17. *In Vitro* Study of Specificity, Uptake and Conversion of 5-ALA to Pp-IX in Co-Culture of 4T1Tumor Cells and NIH/3T3 Cells. **A.** Co-culture of NIH/3T3 cells and 4T1 breast cancer cells. **B.** Fluorescent imaging indicates that there is selective uptake and fluorescence emission in tumorous 4T1 cells only.

Not only can 5-ALA and SpectroPen be used for intraoperative delineation of tumor margins, but this technology can also be employed for photodynamic therapy (PDT), an innovative technique that can be used to eradicate tumor cells (Figure 18). Protoporphyrin-IX can be used as a non-toxic photosensitizer that, upon irradiation and excitation with 630 nm light, results in tumor cell death due to the production of reactive oxygen species through complex biological mechanisms (Dougherty et al., 1978). Thus, 5-ALA and SpectroPen would theoretically enable a surgeon to delineate tumor margins by detecting tumor cells, and to eradicate the cancerous cells through PDT. It should be noted, however, that the extent of PDT-induced tissue damage is limited by light penetration depth (Korbelik, 2006).

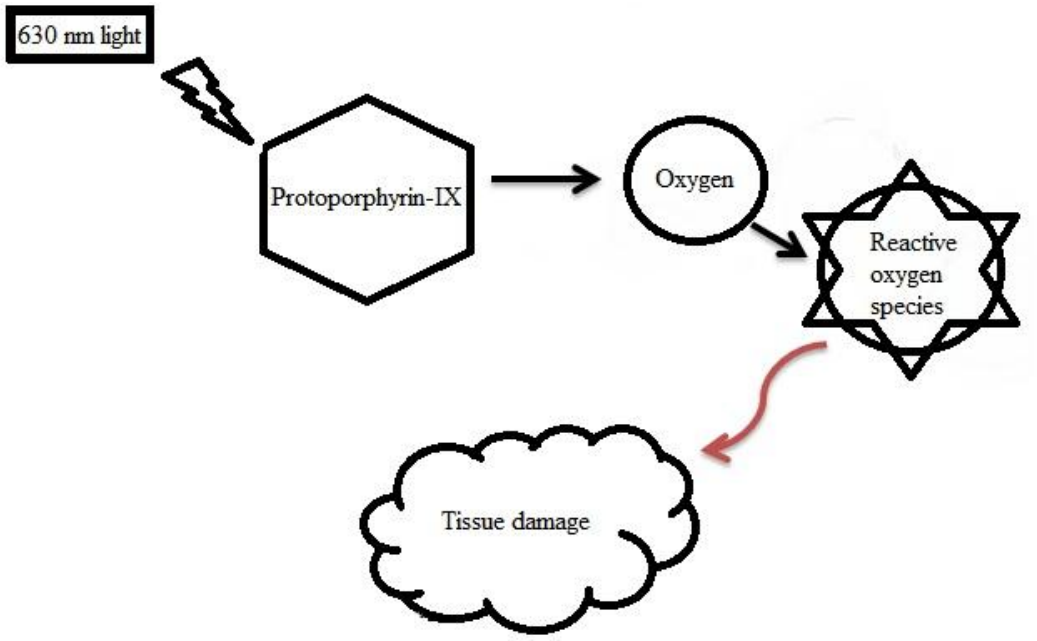

Figure 18. Schematic of Photodynamic Therapy with Pp-IX. Protoporphyrin-IX is a photosensitizer, which, when excited by a 630 nm light, creates reactive oxygen species and free radicals in tissue. PDT initiates cellular apoptosis in tissues in which protoporphyrin-IX accumulates.

Despite the absorption of Pp-IX being around 405 nm, 630 nm light is used for PDT. Even though this 630 nm wavelength is not the maximal absorption for Pp-IX (and thus is not used for FGS, as submaximal absorption would result in weaker fluorescence), the photosensitizer can still be excited and induce the apoptotic pathway in cells. This wavelength, as opposed to the ~400 nm absorption peak for Pp-IX, is used to maximize penetration depth for PDT (Braathen et al., 2007).

A)

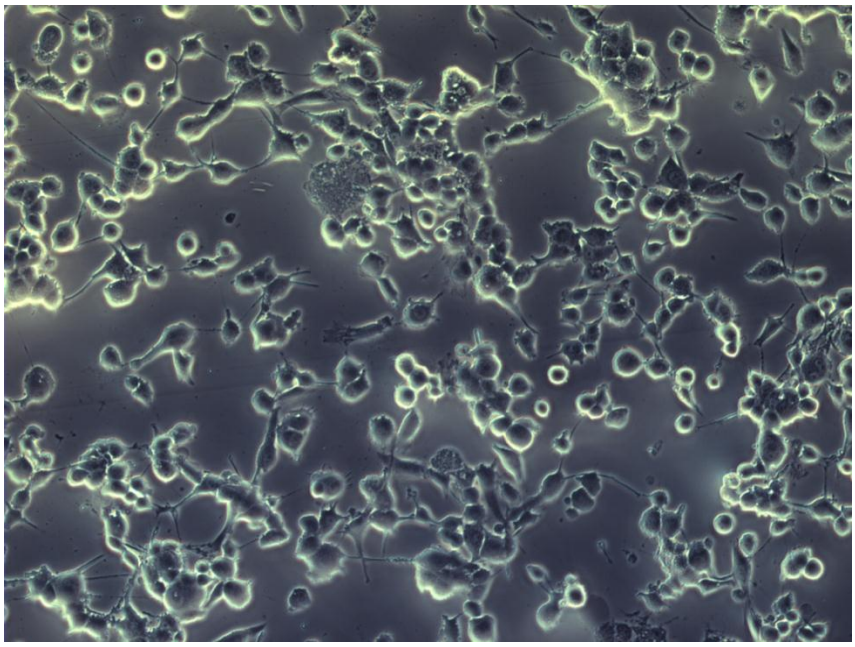

B)

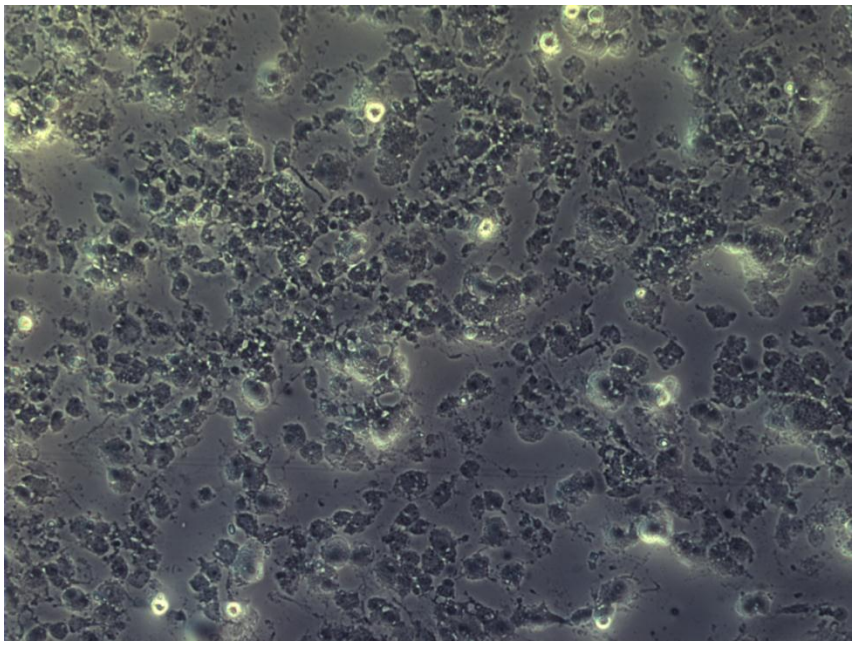

Figure 19. *In Vitro* Study of PDT in U87 EGFR vIII Cells after Incubation and Conversion of 5-ALA to Pp-IX and Irradiation with 630 nm Light for 75 Seconds. **A.** Phase-contrast image of U87 EGFR vIII tumor cells. **B.** Phase-contrast image of U87 EGFR vIII tumor cells following uptake and conversion of 5-ALA to Pp-IX and irradiation for 75 seconds with 630 nm light from SpectroPen. Cytotoxicity appears evident in most cells by observation of the morphological change and the loss of the surrounding halo, characteristic of viable cells; Confirmation of cell death would be achieved via a Calcein-AM/Propidium Iodide cellular viability stain.

Limitations of using 5-ALA as a contrast agent include limited tissue penetration depth of protoporphyrin-IX relative to dyes that emit in the near infrared wavelengths (Smith et al., 2009) as well as possible light sensitivity for a couple of days following administration of 5-ALA to patients (Kennedy et al., 1990).

Relative to ICG, the fluorescence emission of protoporphyrin-IX has a relatively shorter wavelength that results in a reduced ability to detect subsurface tumor tissue. Therefore, this technology would be most ideal for superficial tumor tissue.

Local photosensitization has been reported in patients who have been administered topical dosages of 5-ALA for treatment of superficial skin cancers via PDT, but the photosensitization has been reported to last for only about 48 hours (Kennedy et al., 1990). In addition to such sensitivity to light, PDT has a few additional acute side effects such as pain, and burning sensations in the treated area during exposure to light (Kennedy et al., 2002). Severe ulceration is uncommon, though crusting and skin erosions have been reported in patients treated with PDT for dermatological issues (Ericson et al., 2008). Nevertheless, a clinical trial study by Stummer et al. in Germany reports that the use of 5-ALA for FGS does not cause severe adverse effects or negative side effects in any organ system within a week following surgery (2006).

CONCLUSION

The mobility of the SpectroPen enables surgeons to increase detection sensitivity of tumor cells margins and to more easily delineate tumor cell boundaries. The tendril-like growth arrangements of glioblastoma cells, which diffusely extend into normal tissue, make complete resection of the tumor mass nearly impossible. Therefore, it is of utmost importance to remove as much of the tumor cells as possible in order to prolong the life and survival time of patients. Lacroix et al. demonstrated that 98% glioblastoma cell removal significantly improved the survival time of patients, yet such extensive removal was found to be possible in only about 20% of patients due to the risk involved or technological limitations (2001). As shown here, the use of 5-ALA as a metabolic contrast agent along with SpectroPen, both *in vitro* and *in vivo*, has the potential to significantly increase the occurrence of more complete resection via increased specificity and sensitivity of tumor cell fluorescence. Colditz and Jeffree report that the clinical use of 5-ALA for fluorescence-guided surgery led to a "significant increase in the incidence of complete resection (65% compared to 36%), improved progression-free survival at 6 months (41% compared to 21%), fewer reinterventions, and delayed onset of neurological deterioration," relative to other techniques (2012).

Fluorescence-guided surgery has major implications in assisting surgeons and making the tumor resection process as efficient as possible. This project demonstrates that SpectroPen, coupled with the metabolic contrast agent 5-aminolevulinic acid, has significant advantages for FGS, resulting in greater glioblastoma cell removal while also expediting the process. Visual observation of fluorescence emission only works for larger masses of tumor cells; with the technology presented here, a surgeon would not have to

rely upon such observation of the red, Pp-IX fluorescence because he/she could refer to the corresponding spectrum associated with the particular area of tissue the SpectroPen is placed over. If the characteristic Pp-IX peaks are observed on the spectrum (at ~635 nm and ~704 nm), then the surgeon would know that the tissue possibly contains cancer cells that have accumulated protoporphyrin-ix. The peaks' intensity corresponds to the number of cells fluorescing, the spectrum can be saturated, as when observing the bulk of the tumor mass, or the peaks can be lower, at sub-saturation, which corresponds to a fewer number of fluorescing cells (as should be seen in the tumor margins, where there are fewer tumor cells present). At the detection threshold for the SpectroPen, 2,500 cells, the fluorescence emanating from the tumor cells is not visible with the naked eye and thus reliance upon the spectrum is paramount to determining the presence of tumor cells in areas with fewer cells.

As demonstrated in this project, 5-ALA has a number of advantages over the FDA-approved contrast agents ICG (Figure 20) and fluorescein (Figure 21).

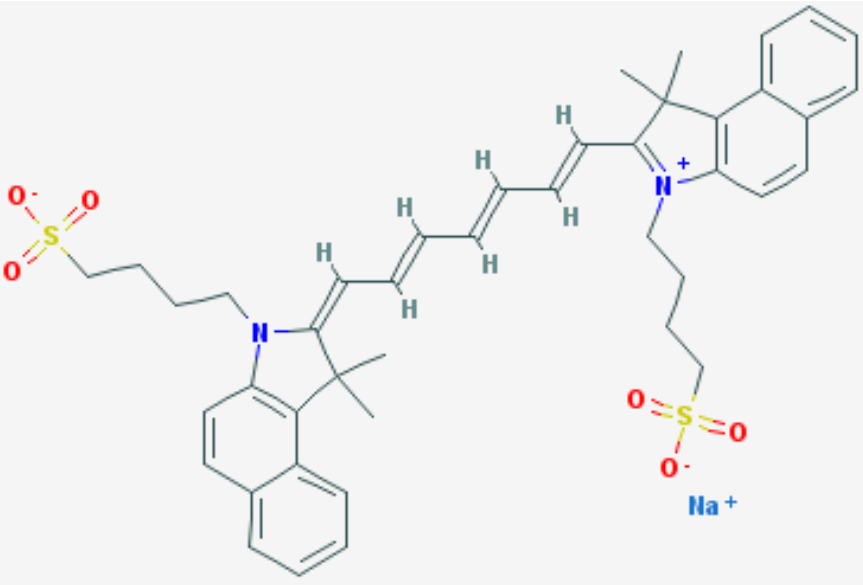

Figure 20. Molecular Structure of Indocyanine Green (ICG); MW = 774.96 g/mol

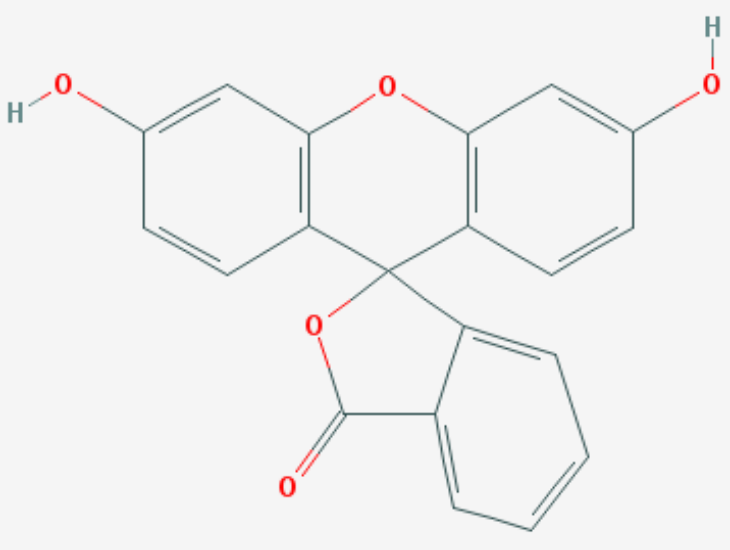

Figure 21. Molecular Structure of Fluorescein; MW = 332.31 g/mol

To reiterate, because 5-ALA is not fluorescent and does not accumulate in tumors via EPR, unlike ICG and fluorescein, there is a lesser probability of non-specific accumulation in off-target organs such as the liver and spleen, two organs that are part of the reticuloendothelial system (Huang et al., 2010). Thus, 5-ALA has a significantly higher signal-to-noise ratio compared to ICG and fluorescein, both of which can more readily result in false positives upon accumulation in normal tissue, from tests done with SpectroPen. The ratio of fluorescence signal intensity to background signal is approximately 100:1 for 5-ALA whereas that for ICG is less than 7:1 (personal communication with Dr. Jian Xu, Nie Group).

With its limited side effects and vast potential, 5-ALA and SpectroPen use for fluorescence-guided surgery has the ability to revolutionize the way surgeons perform tumor resection operations, not only for glioblastoma, but also for a variety of other cancers.

REFERENCES

Aalders MC, Sterenborg HJ, Stewart FA, van der Vange N. (2000) Photodetection with 5-Aminolevulinic acid-induced protoporphyrin IX in the rat abdominal cavity: drug-dose-dependent fluorescence kinetics. Photochem Photobiol. 72(4): 521-525.

Acerbi F, Broggi M, Eoli M, Anghileri E, Cuppini L, Polio B, Schiariti M, Visintini S, Orsi C, Franzini A, Broggi G, Ferroli P. (2013) Fluorescein-guided surgery for grade IV gliomas with a dedicated filter on the surgical microscope: preliminary results in 12 cases. Acta neurochirurgica 155(7):1277-1286.

Braathen LR, Szeimies RM, Basset-Seguin N, Bissonnette R, Foley P, Pariser D, Roelandts R, Wennberg AM, Morton CA. (2007) Guidelines on the use of photodynamic therapy for nonmelanoma skin cancer: an international consensus. International Society for Photodynamic Therapy in Dermatology. J Am Acad Dermatol. 56(1):125-43

Cho YW, Kim YS, Kim IS, Park RW, Oh SJ, Moon DH, Kim SY, Kwon IC. (2008) Tumoral accumulation of long-circulating, self-assembled nanoparticles and its visualization by gamma scintigraphy. Macromolecular Research 16.1: 15-20.

Colditz MJ & Rosalind LJ. (2012) Aminolevulinic acid (ALA)–protoporphyrin IX fluorescence guided tumour resection. Part 1: Clinical, radiological and pathological studies. Journal of Clinical Neuroscience 19.11: 1471-1474.

Daniell WE, Stockbridge HL, Labbe RF, Woods JS, Anderson KE, Bissell DM, Bloomer JR, Ellefson RD, Moore MR, Pierach CA, Schreiber WE, Tefferi A, Franklin GM. (1997) Environmental chemical exposures and disturbances of heme synthesis. Environmental health perspectives 105.Suppl 1: 37.

Dougherty TJ, Kaufman JE, Goldfarb A, Weishaupt KR, Boyle D, Mittleman A. (1978) Photoradiation therapy for the treatment of malignant tumors. Cancer research 38.8: 2628-2635.

Duffner F, Ritz R, Freudenstein D, Weller M, Dietz K, Wessels J. (2005) Specific intensity imaging for glioblastoma and neural cell cultures with 5-aminolevulinic acid-derived protoporphyrin IX. Journal of Neuro-Oncology 71: 107-111.

Ennis SR, Novotny A, Xiang J, Shakui P, Masada T, Stummer W, Smith DE, Keep RF. (2003) Transport of 5-aminolevulinic acid between blood and brain. Brain research 959.2: 226-234.

Ericson MB, Wennberg AM, Larkö O. (2008) Review of photodynamic therapy in actinic keratosis and basal cell carcinoma. Therapeutics and clinical risk management 4.1: 1.Tuchin, 2000

Gates DM. (1980) Biophysical Ecology. New York: Springer-Verlag.

Hansen DA, Spence AM, Carski T, Berger MS. (1993) Indocyanine green (ICG) staining and demarcation of tumor margins in a rat glioma model. Surgical neurology 40.6: 451-456.

Huang X, Peng X, Wang Y, Shin DM, El-Sayed M, Nie S. (2010) A reexamination of active and passive tumor targeting by using rod-shaped gold nanocrystals and covalently conjugated peptide ligands. ACS nano 4.10: 5887-5896.

Jouyban A., Soltani S. (2012) Blood Brain Barrier Permeation. Toxicity and Drug Testing.

Kennedy JC & Pottier RH. (1992) New trends in photobiology: endogenous protoporphyrin IX, a clinically useful photosensitizer for photodynamic therapy. Journal of Photochemistry and Photobiology B: Biology 14.4: 275-292.

Kennedy JC, Pottier RH, Pross DC. (1990) Photodynamic therapy with endogenous protoporphyrin: IX: basic principles and present clinical experience. Journal of Photochemistry and Photobiology B: Biology 6.1: 143-148.

Korbelik, Mladen. (2006) PDT-associated host response and its role in the therapy outcome. Lasers in surgery and medicine 38.5: 500-508.

Kosaka N, Mitsunaga M, Longmire MR, Choyke PL, Kobayashi H. (2011) Near infrared fluorescence-guided real-time endoscopic detection of peritoneal ovarian cancer nodules using intravenously injected indocyanine green. International Journal of Cancer 129.7: 1671-1677.

Lacroix M, Abi-Said D, Fourney DR, Gokaslan ZL, Shi W, DeMonte F, Lang FF, McCutcheon IE, Hassenbusch SJ, Holland E, Hess K, Michael C, Miller D, Sawaya R. (2001) A multivariate analysis of 416 patients with glioblastoma multiforme: prognosis, extenet of resection, and survival. J Neurosurg. 95(2): 190-198.

Mohs AM, Mancini MC, Singhal S, Provenzale JM, Leyland-Jones B, Wang MD, Nie S. (2010) Hand-held spectroscopic device for in vivo and intraoperative tumor detection: contrast enhancement, detection sensitivity, and tissue penetration. Analytical chemistry 82(21): 9058-9065.

Navone NM, Polo CF, Frisardi AL, Batlle AM. (1991) Mouse mammary carcinoma porphobilinogenase and hydroxymethylbilane synthetase. Comparative Biochemistry and Physiology Part B: Comparative Biochemistry 98.1: 67-71.

Novotny A., Xiang J, Stummer W, Teuscher NS, Smith DE, Keep RF. (2000) Mechanisms of 5-Aminolevulinic Acid Uptake at the Choroid Plexus. Journal of neurochemistry 75.1: 321-328.

Richards-Kortum R, Sevick-Muraca E. (1996) Quantitative optical spectroscopy for tissue diagnosis.Annu Rev Phys Chem. 47:555–606.

Rodriguez L, Batlle A, Di Venosa G, Battah S, Dobbin P, MacRobert AJ, Casas A. (2006) Mechanisms of 5-aminolevulic acid ester uptake in mammalian cells. British journal of pharmacology 147.7: 825-833.

Rubino GF & Rassetti L. (1966) Porphyrin metabolism in human neoplastic tissues. Panminerva Med 8: 290–292.

Shinoda J, Yano H, Yoshimura SI, Okumura A, Kaku Y, Iwama T, Sakai N. (2003) Fluorescence-guided resection of glioblastoma multiforme by using high-dose fluorescein sodium. J Neurosurg. 99: 597-603.

Singh Y, Gao D, Gu Z, Li S, Stein S, Sinko PJ. (2011) Noninvasive detection of passively targeted poly (ethylene glycol) nanocarriers in tumors. Molecular pharmaceutics 9.1: 144-155.

Smith, AM, Mancini MC, Nie S. (2009) Second window for in vivo imaging. Nature nanotechnology 4.11: 710.

Stummer W, Pichlmeier W, Meinel T, Wiestler OD, Zanella F, Reulen HJ, ALA-Glioma Study Group. (2006) Fluorescence-guided surgery with 5-aminolevulinic acid for resection of malignant glioma: a randomised controlled multicentre phase III trial. The lancet oncology 7.5: 392-401.

Stummer W, Novotny A, Stepp H, Goetz C, Bise K, Reulen HJ. (2000) Fluorescence-guided resection of glioblastoma multiforme by using 5-aminolevulinic acid-induced porphyrins: a prospective study in 52 consecutive patients. J Neurosurg. 93(6): 1003-1013.

Stupp R, Mason WP, van den Bent MJ, Weller M, Fisher B, Taphoorn MJ, Belanger K, Brandes AA, Marosi C, Bogdahn U, Curschmann J, Janzer RC, Ludwin SK, Gorlia T, Allgeier A, Lacombe D, Cairncross JG, Eisenhauer E, Mirimanoff RO, European Organisation for Research and Treatment of Cancer Brain Tumor and Radiotherapy Groups, National Cancer Institute of Canada Clinical Trials Group. (2005) Radiotherapy plus concomitant and adjuvant temozolomide for glioblastoma. N Engl J Med. 352(10): 987-996.

Tuchin V. (2000) Tissue optics: light scattering methods and instruments for medical diagnosis.Bellingham, Washington: SPIE – The International Society for optical Engineering.

Vahrmeijer AL, Hutteman M, van der Vorst JR, van de Velde CJ, & Frangioni JV (2013) Image-guided cancer surgery using near-infrared fluorescence. Nature Reviews Clinical Oncology 10: 507-518.

Van Meir EG, Hadjipanayis CG, Norden AD, Shu HK, Wen PY, Olson JJ. (2010) Exciting new advances in neuro-oncology: The avenue to a cure for malignant glioma. CA: A cancer journal for clinicians 60(3): 166-193.

Weisstein, EW. "Least Squares Fitting." From *MathWorld*--A Wolfram Web Resource. http://mathworld.wolfram.com/LeastSquaresFitting.html